Journal of the European Ceramic Society 22 (2002) 495–503

www.elsevier.com/locate/jeurceramsoc

Hydration of refractory oxides in castable bond systems—I: alumina, magnesia, and alumina–magnesia mixtures

K. Ghanbari Ahari, J.H. Sharp*, W.E. Lee

Department of Engineering Materials, University of Sheffield, Mappin Street, Sheffield S1 3JD, UK

Received 2 November 2000; received in revised form 20 April 2001; accepted 28 April 2001

Abstract

Isothermal conduction calorimetry (ICC) of hydratable alumina and reactive magnesia revealed that alumina was partially hydrated to bayerite while magnesia was fully hydrated to brucite after curing for 22 h at 20 and 30 °C. Hydration of Al_2O_3–MgO mixtures led to formation of a hydrotalcite-type hydrate accompanied by total heat evolution of ≈600 kJ/kg. This level of heat evolution from the mixed oxide was comparable with that from the hydration of magnesia, but much of it was released later in the hydration process. Such a large and delayed heat evolution might explain serious problems sometimes observed when mixed Al_2O_3–MgO bond systems are used in castable refractories.

Keywords: Al_2O_3; Calorimetry; Castable refractories; MgO; Refractories

1. Introduction

The most common bond system in monolithic refractories is based on calcium aluminate cement (CAC) that sets via hydration reactions at ambient temperatures. However, the presence of lime in the matrix from CAC leads to poor high-temperature properties since it fluxes with any silicates present in the refractory or slag. Consequently, alternative lime or cement-free systems have been developed[1] often based on transitional aluminas such as χ- or ρ-Al_2O_3. Once installed and set these refractories are dried and fired to develop ceramic bonds. Addition of fine, reactive magnesia may lead to formation of refractory spinel type ceramic bonds.

Alumina–magnesia based castable refractories have superior high temperature corrosion resistance than competing materials, such as high alumina castables and have found applications in steel ladles, RH degasser and cement kilns. Recent investigations[2] have shown that alumina-magnesia spinel castables could be a viable alternative to fusion cast and silica refractories in glass melting furnaces using Oxy-Fuel technology. The crystal structure of magnesium aluminate spinel can accommodate high levels of deleterious elements such as Fe and Mn from slags without loss of structural integrity.[3] Static cup tests, dynamic rotary slag tests and field trials in steel ladles have shown that spinel-based alumina-rich castables have excellent slag resistance.[4,5] Spinel ($MgAl_2O_4$) is easily formed in situ from mixtures of fine reactive magnesia and hydratable alumina included in the formulation of castable mixes.[6]

Several technological problems arise on adding MgO to castable systems. While refractory grade magnesias have larger crystallite sizes and lower specific surface area than reactive grades, and so are more resistant to hydration at casting and drying temperatures (e.g. up to 110 °C), they may still undergo unpredictable hydration. This can lead to violent high temperature reactions, e.g. with water vapour from the dehydration of refractory cements.[7] Hydration of magnesia in a hardened cast body can cause swelling and subsequent cracking. Consequently, it would be desirable that the magnesias used in castable formulations hydrate on mixing with water and in subsequent curing stages rather than later in the process. Some difficulties on placement of mixes containing reactive MgO have also been reported.[7] Sandberg et al.[8] added 1.5 wt.% reactive magnesia to a cement-free spinel-alumina based mix containing 6% fumed silica and produced samples with reasonable green strength.

* Corresponding author. Tel.: +44-114-222-5504; fax: +44-114-222-5943.

E-mail address: j.h.sharp@sheffield.ac.uk (J.H. Sharp).

0955-2219/02/$ - see front matter
PII: S0955-2219(01)00299-0

The objectives of this calorimetry study were to measure the rate and total amount of heat evolution on hydration of the pure oxides, binary and ternary mixtures of hydratable alumina, reactive magnesia and fumed silica. Combinations of these oxides can lead to formation of high temperature resistant compounds, such as spinel, mullite and forsterite. ICC indicates the temperature rise on setting of castables containing such reactive mixtures in their bond systems. Also the nature of the heat evolution might be more precisely correlated to the setting and strength development in castables with different bonding systems. This paper describes a calorimetric study of hydration in hydratable alumina, reactive magnesia, and alumina-magnesia mixtures which may be used in the bond systems of spinel-based refractory castables. Results on alumina-fumed silica and magnesia-fumed silica mixtures will be reported later.

2. Experimental

Mixtures of hydratable alumina (Actibond 102) from Alcan Chemicals Ltd, and magnesium oxide from Aldrich Chemical Co. (catalogue No. 30,774-2), were hydrated for up to 22 h at 20 and 30 °C in a conduction calorimeter. Percentages and ratios are on a weight basis unless otherwise stated. According to the supplier's data, loss on ignition (LOI) of alumina was 4.5%, its Na_2O content 0.45%, its specific surface area (SSA) 260 m^2/g, and median particle size 6 μm. Titration purity of the magnesia was 96–100.5% and its LOI 10% maximum.

A conduction calorimeter from Wexham Developments, based on the Forrester[9] design, was used to hydrate the samples. Samples were located in a calorimeter cell, kept at constant test temperature (±0.1 °C) inside a water bath. This type of calorimeter measures the rate of heat evolution from a hydrating material and allows accurate measurement of the total heat evolved at a particular time during hydration. Five grammes of as-received pure oxides or mixes with varying Al_2O_3:MgO ratio (Tables 1 and 2) were externally mixed with 4 cm^3 distilled water in a polyethylene bag tied with aluminium tape. Mixing samples internally (i.e. injecting water while the powder sample is inside the cell) is possible, but was not done regularly due to the small sample size (1 g) needed which was insufficient to characterise the hydration products. Nonetheless, a few experiments were conducted using the internal mixing route to determine the rate and total amount of heat evolution from the earliest stages of hydration. The alternative process of external mixing with water, spatulation and transfer to the calorimeter to start recording the heat evolution data usually took 5–7 min. Under these circumstances, because the cell is sealed the water vapour pressure rapidly rises to reach 100% relative humidity.

Table 1
Sample composition (wt.%) and total heat evolution on hydration (kJ/kg) with time at 20 °C, using external mixing

Alumina	Magnesia	1 h	5 h	10 h	15 h	20 h
100	0	40	72	99	121	141
75	25	49	123	153	168	180
50	50	49	109	159	224	299
35	65	60	147	340	462	513
25	75	53	278	419	466	488
10	90	52	232	301	329	345
0	100	38	190	249	276	290

Table 2
Sample composition (wt.%) and total heat evolution on hydration (kJ/kg) with time at 30 °C, using external mixing

Alumina	Magnesia	1 h	5 h	10 h	15 h	20 h
100	0	40	110	145	170	180
90	10	55	134	165	180	192
75	25	65	150	175	195	215
50	50	84	188	368	487	505
35	65	60	440	548	573	586
10	90	45	145	201	218	222
0	100	40	150	199	217	220

A typical ICC trace on using internal mixing consists of an immediate exothermic wetting peak followed by a dormant period with little or no heat evolution and then one or more hydration peaks appear depending on the composition and the reactions involved.[10] Associated with the external mixing route is a lack of thermal equilibrium during the first 1 h of the experiment, which may cause the ICC trace to deviate from the base line. This deviation is exothermic if the ambient temperature is greater than the test temperature and endothermic if it is less. The wetting peak occurs as soon as material comes into contact with water and it can be largely located within the non-equilibrium period in the external mixing route. Consequently, the ICC output for the first hour is a complex summation of heats from several causes, and these results, particularly from materials with a low level of heat evolution on hydration such as fumed silica or highly hydraulic materials such as fine crystalline magnesia, can be difficult to interpret. Using internal mixing can reduce the problems giving a better measurement of heat evolution from the early stages of hydration.

Acetone quenching was used to arrest hydration. Quenched pastes were dried inside a fume hood for 24 h and also in an oven for another 24 h at 80 °C and stored in a desiccator prior to further characterisation. Phase analysis was performed by X-ray diffraction on the starting oxides and hydrated materials using a Philips PW-1730 diffractometer, operating at 50 kV and 30 mA. Scanning was carried out over a range of 10 to 70° (2θ at step size of 0.02°, speed of 2°/min) using Cu K_α radiation. Generated spectra were compared with JCPDS cards 20–11 (bayerite), 7–324 (gibbsite), 4–829 (magnesium

oxide), 7–239 (brucite) and 22–700, 41–1428 (hydrotalcite). Crystallite sizes were determined by peak broadening measurements and applying the Debye-Scherer equation. The specific surface area of the powders was calculated applying the BET equation to data obtained using a Micromeritics isothermal gas absorption analyser. Thermogravimetry (TG) was conducted in air using a Stanton Redcroft TG760 unit, with a 5 K/min heating rate up to 550 °C. A Micromeritics, Atlanta (Pore Sizer 9320) mercury porosimeter was used to investigate the pore structure of the hydratable alumina. Scanning electron microscopy (SEM) and Environmental SEM were used to study the microstructure of the starting materials and the hydration products, respectively.

3. Results and preliminary discussion

3.1. Characterisation of the raw materials

Hydratable alumina formed from the Bayer process, is a lightly calcined gibbsite comprising predominantly X-ray amorphous, metastable, transitional alumina(s). The average particle size of the pseudomorphic agglomerates was ≈15 μm and they are highly porous (Fig. 1a). The pore structure of this hydratable alumina was shown by mercury porosimetry (Fig. 2) to consist of intra- and inter-agglomerate pores with mean diameters of ~20 and ~2 μm, respectively. The manufacturer's quoted SSA is ~260 m^2/g. The agglomerates were hard and a bulk density of only ~1.30 g/cm^3 was obtained after applying 180 MPa pressure. Consequently, these agglomerates are unlikely to disperse on mixing with water.

The magnesium oxide was produced by light calcination of brucite and contains fine ~12 nm crystallites with SSA ~90 m^2/g. XRD indicated it was single phase. TG showed a weight loss of 1.44% after heating to 550 °C at 5 K/min, which is mainly related to free water. The powder morphology (Fig. 1b) consisted of agglomerates of nm scale crystallites with a complicated pore structure.

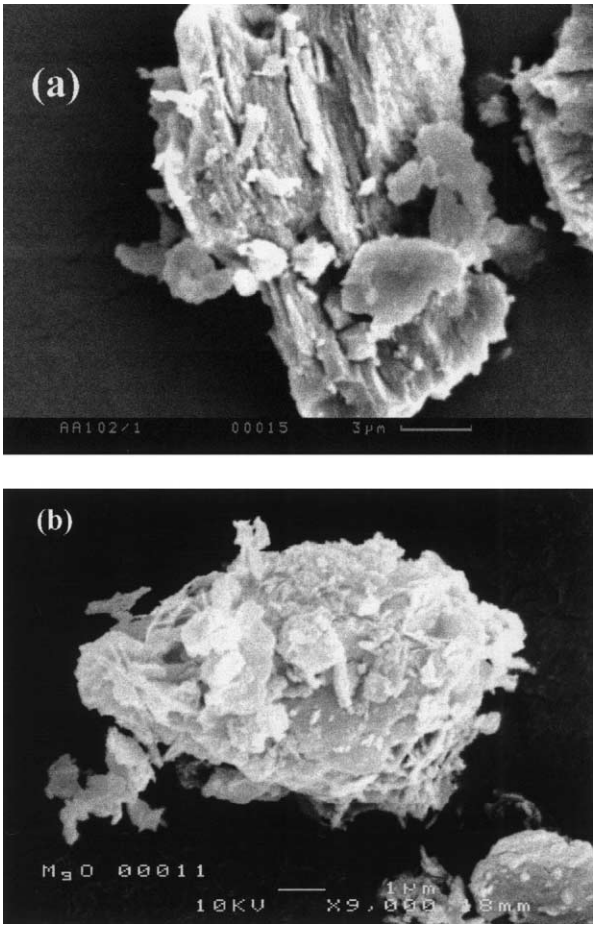

Fig. 1. Secondary electron SEM images of agglomerates (a) hydratable alumina and (b) magnesium oxide (courtesy of K.J. Norton-Berry, University of Sheffield).

3.2. Hydration studies using ICC

Hydration of alumina, magnesia and their mixture (35:65 of Al_2O_3:MgO) as followed by ICC using external and internal mixing is shown in Figs. 3a and b, respectively. On external mixing no heat evolution was detected for a certain time, although once it began a massive exothermic peak was observed, which should not be mistaken as merely a wetting peak. Surprisingly, the duration of the non-data collection period was different for each material but remained unaltered for a particular material on repeating the experiment. Comparison of the internal and external mixing ICC curves shows that in the highly reactive magnesia more than 50% of the total heat was missed on external mixing. Alumina was not as highly reactive as the magnesia and little heat was evolved at the initial stage so that similar results were obtained using internal and external mixing. Results from the two mixing procedures for Al_2O_3:MgO ratio of 35:65 also showed little variation. As this

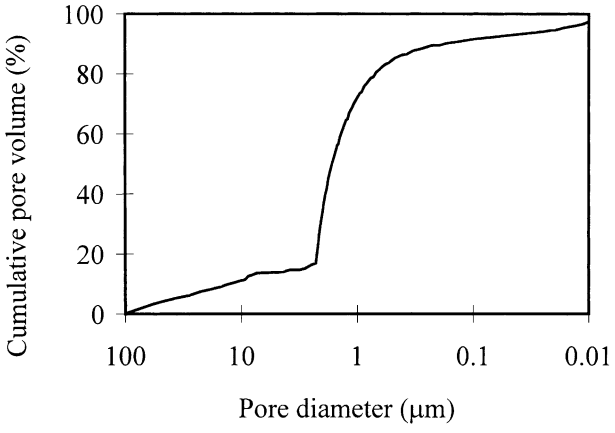

Fig. 2. Pore size distribution of hydratable alumina.

mix contained 65% MgO it might be expected that external mixing would lead to lower total heat evolution. However, it appears that mixing alumina with magnesia delays the hydraulic activity of magnesia, while the presence of magnesia appears to accelerate alumina hydration so that the total heat evolution observed is close for both mixing procedures. These figures are much higher than the simple summation of the heats from the hydration of the individual oxides due to formation of a new hydration product that is discussed in more detail below.

As the total heats of hydration from the first hour for alumina and its mixtures with magnesia (up to 75% MgO) using both external and internal mixing were comparable, the external route was employed for further studies since it provided more hydration product for further characterisation and was experimentally more straightforward to carry out. In practice castables may be installed up to 40 min after water addition so that the ICC results from the external mixing route are commercially relevant. Because the heat evolved during the initial stages of hydration has been excluded, the total heat evolution reported will be lower than that actually evolved.

3.3. Hydration of the individual oxides

When the alumina was mixed with water, heat evolution could be detected by hand prior to insertion of the sample in the calorimeter (using the external mixing procedure). ICC (Fig. 4) revealed that the rate of heat evolution (during the initial stages of hydration) and the total heat evolved at 30 °C were higher than at 20 °C for the duration of the experiment (20 h). Following the early stages of the experiment, alumina showed a series of hydration peaks (Fig. 4a) whose position was delayed to longer times at the lower test temperature. As the alumina had a poorly developed crystal structure and was probably composed of numerous transitional aluminas, the hydration peaks are likely to be related to the existence of complex hydration intermediates associated with its complicated crystal and pore structures (Figs. 1a and 2). XRD (Fig. 5a) revealed that the principal crystalline hydration product was bayerite, $Al(OH)_3$, consistent with the results of Ma and Brown.[11] The stoichiometric water content of bayerite is 34.6%. TG (Fig. 6a) revealed that the product of both hydration temperatures (20 and 30 °C) showed a weight loss of 15–20%, i.e. less than half of the possible total. Since the

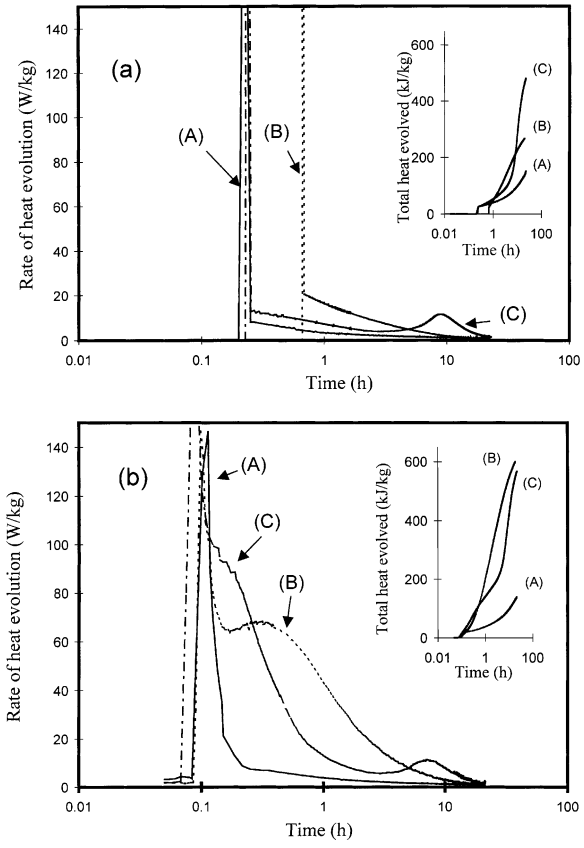

Fig. 3. ICC of pure alumina (A), magnesia (B), and alumina–magnesia mixture [Al_2O_3:MgO (35:65)] (C) at 20 °C using (a) external and (b) internal mixing.

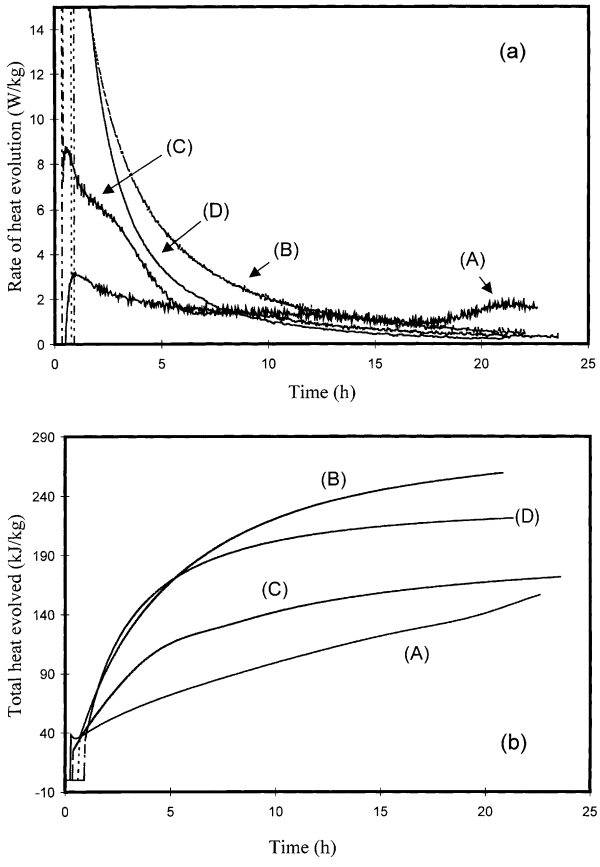

Fig. 4. ICC curves demonstrating hydration of alumina and magnesia at test temperatures of 20 and 30 °C using external mixing (a) rate of heat evolution, (b) total heat evolved. (A) Alumina at 20 °C, (B) magnesia at 20 °C, (C) alumina at 30 °C, (D) magnesia at 30 °C.

heat evolved after 20 h at 20 and 30 °C is 140–180 kJ/kg (Tables 1 and 2) the total heat of reaction on complete hydration of alumina is estimated to be of the order of 400 kJ/kg.

The calorimeter did not respond for approximately one hour when using the external mixing procedure on hydration of MgO (Fig. 4) at both test temperatures. Over this period more than 50% of the total heat from the hydration was not detected. Data collection had therefore started somewhere in the middle of the hydration process so that the heat from the exothermic wetting peak and early stages of hydration had been lost. Data from the internal mixing route revealed that hydration of MgO started almost immediately after wetting and thus showed no dormant period and gave rise to a huge asymmetric hydration peak (Fig. 3b). With external mixing only part of this peak has been detected. The total heat evolution at 20 °C was greater than at 30 °C (Tables 1 and 2) implying that the portion of undetected heat evolution at 30 °C is higher than at 20 °C. The weight loss determined from TG (Fig. 6a) from both samples was similar and XRD suggests that they were fully hydrated at both test temperatures. The only crystalline hydration product of MgO is brucite, $Mg(OH)_2$, although a small XRD peak at 29.4°2θ (d = 3.035Å) was also observed, which might be related to the presence of some calcite ($CaCO_3$) impurity (Fig. 5b). The calculated water content of brucite is 30.9% and TG revealed a total weight loss including free moisture of up to 35% so that hydration of MgO at both temperatures was close to completion. These experiments suggest that the heat of hydration of MgO is at least 600 kJ/kg.

3.4. Hydration of alumina-magnesia mixtures

The amount of heat evolved after various times in all the ICC runs carried out using external mixing at 20 and 30 °C are given in Tables 1 and 2. The total heat evolved on hydration of alumina and magnesia mixtures at 20 °C with Al_2O_3:MgO ratio ~35:65 (Fig. 7) is much higher than that from the pure oxides (Fig. 4b). XRD of the hydration products revealed that, in addition to brucite, a hydrotalcite type hydrate was formed during hydration (Fig. 5c). The pattern is similar to JCPDS card 22–700 with slight (0.05°) displacement of the peaks' positions towards higher 2θ values. Hydrotalcite is a hydrated hydroxycarbonate of magnesium and aluminium, the

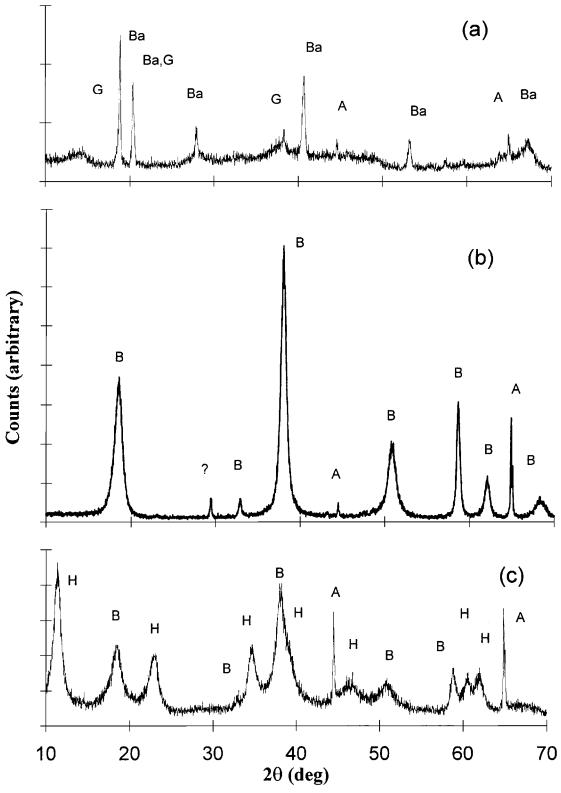

Fig. 5. XRD of samples hydrated for 22 h at 30 °C, (a) alumina, (b) magnesia and (c) alumina–magnesia mixture [Al_2O_3:MgO (35:65)]. G = gibbsite, Ba = bayerite, B = brucite, H = hydrotalcite, A = aluminium (sample holder).

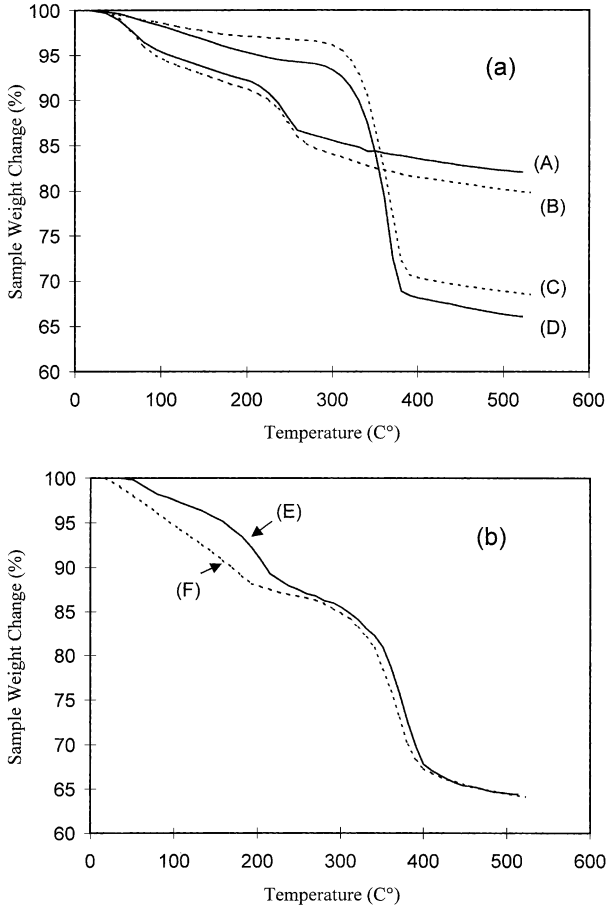

Fig. 6. TG demonstrating dehydration sequences of the samples hydrated at 20 and 30 °C, (a) individual magnesia and alumina (b) alumina–magnesia mixtures with Al_2O_3:MgO ratio of 35:65. (A) alumina, 20 °C, (B) alumina, 30 °C, (C) magnesia, 30 °C, (D) magnesia, 20 °C, (E) mixture, 30 °C (F) mixture, 20 °C.

ideal formula of which is $Mg_6Al_2CO_3(OH)_{16}.4H_2O$, although the Mg:Al ratio in natural hydrotalcite can vary from 3:1 to 2:1.[12] The variable stoichiometry almost certainly explains the observed peak shift. Several investigators[13–15] have studied the hydrotalcite structure and its thermal decomposition. Thermal decomposition studies of the hydration product by TG (Fig. 6b) showed a similar weight loss pattern to that reported by Pesic et al.[14] The first major weight loss occurs around 220 °C, from loss of interlayer water and the second major loss occurs around 360 °C, due to loss of the (OH) and (CO_3) groups. In hydrotalcite with the ideal formula the interlayer water content is 11.96%, the (OH) content is 23.92% and the (CO_3) content is 7.31%. TG results of this work (when corrected for free moisture content) are in good agreement with the above figures; bearing in mind that the (CO_3) content of the samples in this study should be much lower than theoretical.

A distinctive hydration peak appeared on the ICC curves, shown in Fig. 7a, of samples with higher hydrotalcite content. Fig. 7b demonstrates the total heat evolution with time for such samples (e.g. Al_2O_3:MgO ratio of 25:75, 35:65, 50:50) hydrated at 20 °C. XRD revealed that these samples contained high levels of hydrotalcite. ICC of alumina at this temperature (Fig. 4a) showed two distinct peaks, one was after curing for ~1 h and the other after ~22 h. By adding MgO to alumina the position of the second peak was observed at shorter times and eventually a single peak was attained for pure MgO. The position of the first peak of alumina remained almost unchanged up to 75% MgO addition.

Representative ICC results from hydration of some compositions at 30 °C are shown in Fig. 8. The highest total heat evolution, approaching 600 kJ/kg after 22 h hydration, was for samples with an Al_2O_3:MgO ratio of 35:65, similar to the results obtained at 20 °C. At the higher test temperature the hydration was faster, as illustrated for compositions with Al_2O_3:MgO ratio of 50:50 and 35:65 (Fig. 9). Increasing the temperature from 20 to 30 °C caused the main hydration peak to move towards shorter times (Fig. 9a). Hydration of (50:50) at 20 °C demonstrated that the relationship between total heat evolved and time was almost linear. After 22 h there was little change in reaction rate compared to the other three

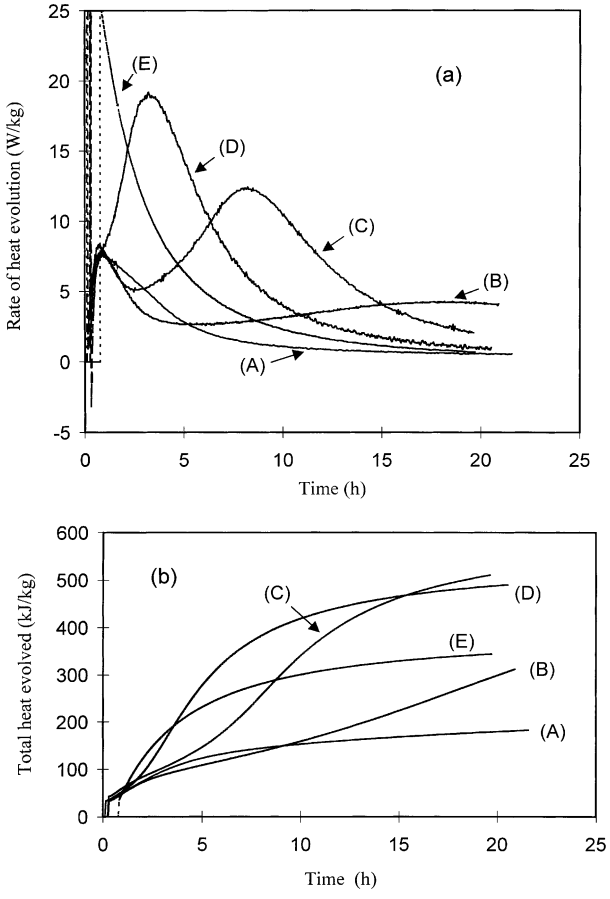

Fig. 7. ICC curves demonstrating hydration of alumina–magnesia mixtures at 20 °C, using external mixing (a) rate of heat evolution, (b) total heat evolved. Al_2O_3:MgO ratios: (A) 75:25, (B) 50:50, (C) 35:65, (D) 25:75, (E) 10:90.

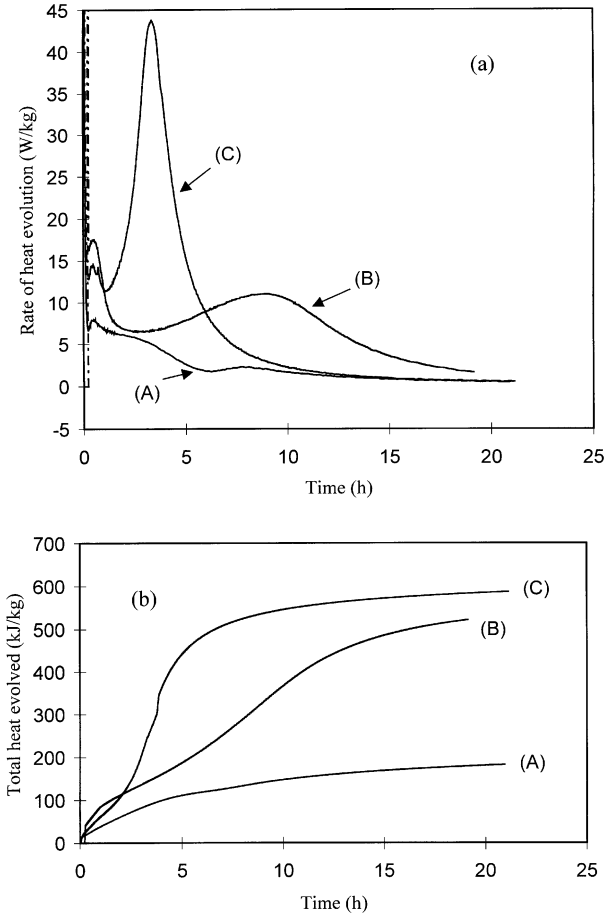

Fig. 8. ICC curves demonstrating hydration of alumina-magnesia mixtures at 30 °C, using external mixing (a) rate of heat evolution, (b) total heat evolved. (A) alumina, (B) Al_2O_3:MgO ratio of 50:50, (C) Al_2O_3:MgO ratio of 35:65.

samples in which reaction rate had slowed (Fig. 9b). Related to this is the fact that the extent of mixing of the samples is not ideal. This is indicated by the observation of brucite along with hydrotalcite in mixed samples containing up to Al_2O_3:MgO ratio of 75:25. Increasing the temperature from 20 to 30 °C had no effect on the type of hydration product. Brucite and bayerite were the hydration products of the pure oxides, while hydrotalcite was the dominant product from the relevant mixtures.

Fig. 10 has been constructed from the ICC data obtained during the hydration of mixtures of alumina and magnesia, including the pure end-members, based on the heat evolved after various time periods up to 20 h. At all compositions the amount of heat evolved increased with increasing time of hydration, but, more importantly, it varied significantly with compositions containing 60–70% MgO. Hydrotalcite and brucite were the hydration products of the mixtures. XRD showed that the amount of both phases increased as the MgO content of the mixes was increased.

Hydration of pure alumina and pure magnesia (depending on test temperature) showed a total heat evolution of 140–180 and 220–300 kJ/kg respectively using the external mixing route. Formation of hydrotalcite from hydration of samples with Al_2O_3:MgO ratio of 35:65 is associated with higher heat evolution (~600 kJ/kg) compared to the pure oxides. This level of excessive heat evolution almost certainly can lead to serious installation difficulties in castables containing similar bond compositions, particularly, in the control of the drying step.

4. Further discussion

ICC of alumina revealed a series of hydration peaks which may be attributed to the complex morphology of the alumina agglomerates (Fig. 1a) and possible coexistence of transition aluminas. Inter- and intra-agglomerate open pores and inter-grain closed pores are present due to its derivation from precipitated Bayer process gibbsite with which it is pseudomorphic.[16] On calcination the higher density of Al_2O_3 compared to that of gibbsite means that, to retain the same volume in the pseudomorphs, pores must be created within them. These remain in alumina (Actibond 102) and are penetrated

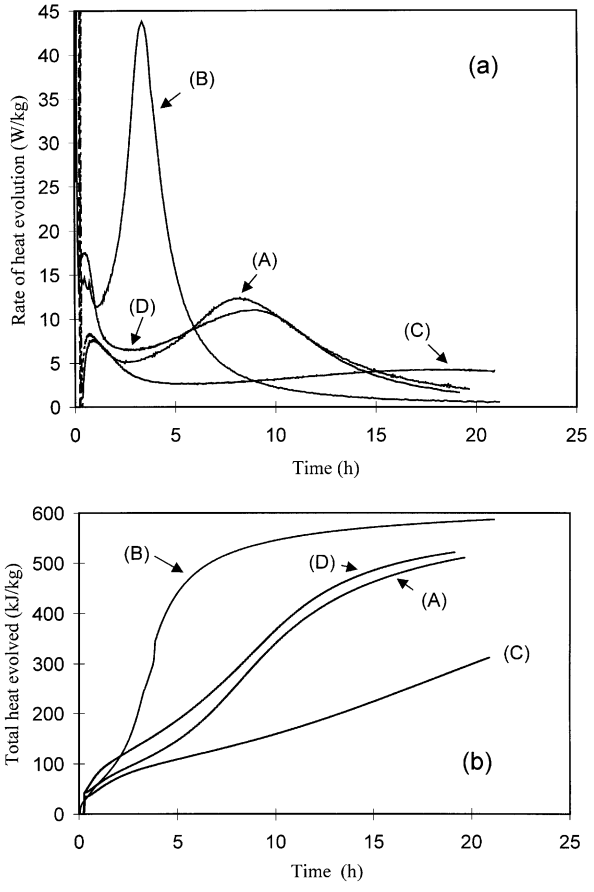

Fig. 9. ICC curves comparing hydration of alumina–magnesia mixtures at 20 and 30 °C, using external mixing (a) rate of heat evolution, (b) total heat evolved. (A) 35:65, 20 °C, (B) 35:65, 30 °C, (C) 50:50, 20 °C, (D) 50:50, 30 °C.

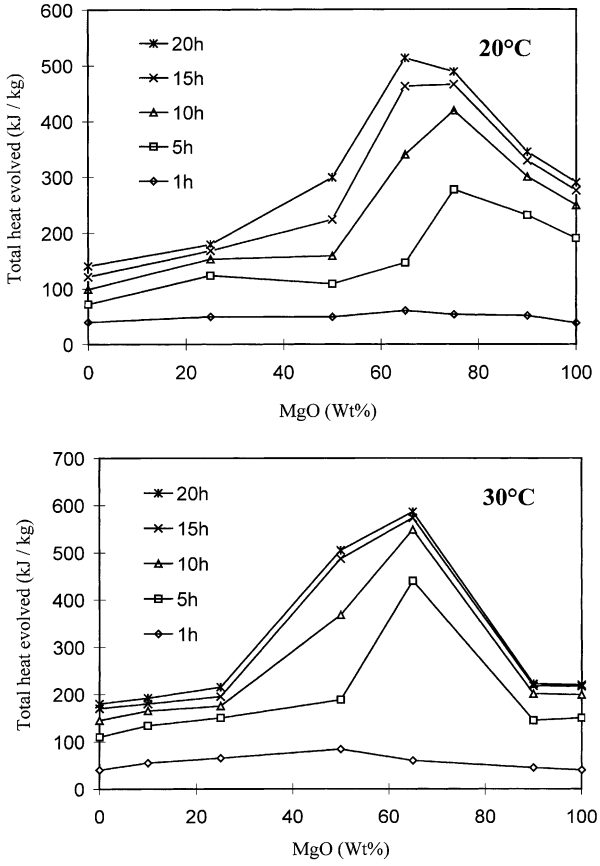

Fig. 10. Total heat evolution from mixtures with varying Al_2O_3:MgO ratios hydrated at 20 and 30 °C, using external mixing.

sequentially by water leading to the appearance of the various relevant hydration peaks. Hydration is accelerated by increasing the test temperature, most likely due to increasing the solubility and altering the diffusion coefficients of those diffusing ions in favour of hydration. Hydration was only ~45% of that possible after 22 h at 20 or 30 °C, suggesting that latent hydraulic activity would continue. The hydration mechanism for alumina suggested by the results of this study involves endothermic dissolution of a layer of solid material in water forming a viscous gel which slows down the hydration process. Alternate precipitation of the hydration product from the gel and further dissolution of fresh material in diluted gel continues during the course of hydration. Such a mechanism is well known on hydration of transitional aluminas obtained by flash calcination,[17] and either individually or in concert with the sequential penetration of water in different pore structures could be responsible for the particular ICC trace of the alumina under investigation.

The magnesia used in this study is a chemically-derived fine powder whose hydration was almost complete after 22 h at 20 and 30 °C. It shows an unusual ICC trace with a massive skewed hydration peak at ~1 h. The vigour of its hydration means that its morphology was less significant than that of alumina. This might be related to its higher solubility and widespread formation of nuclei resulting in little space for growth in the course of hydration, as suggested by Environmental SEM examination of brucite and MgO.[18]

The current work has revealed that a hydrotalcite-type hydrate forms on hydrating mixtures of alumina with reactive magnesia. Hydrotalcite-type phases are structurally related to brucite, where some of the Mg^{2+} ions are replaced by tri-positive ions, typically Al^{3+} or Fe^{3+}, and the charge is balanced by anions such as CO_3^{2-} and OH^- which, together with H_2O molecules, occupy interlayer sites. Many other phases of this type are known, as other cations of similar size can replace the Mg^{2+} or Al^{3+} or both and other anions can replace the CO_3^{2-}. Hydroxyl ions can replace the CO_3^{2-} in hydrotalcite, giving meixnerite, which is easily carbonated.[19]

The positions of the maxima with respect to chemical composition and the total amounts of heat evolved due to the formation of hydrotalcite at 20 and 30 °C are similar (Fig. 10). Formation of hydrotalcite facilitated the hydration of the mixed oxides and the existing alumina has been almost fully consumed in such samples at 20 and 30 °C. Mixed bond systems such as those examined in this study have good potential for use in spinel-based castable systems containing no calcium aluminate cement and no fumed silica. Dehydration of hydrotalcite (with its layered double hydroxide structure) leaves a micro-porous microstructure which might aid the castable drying process both by allowing escape of vapours and by accommodating any dehydration products. In situ spinel formation at high temperatures is accompanied by a volume expansion[20] which might also be beneficially accommodated by this porous network.

The observed doubling of the total heat evolved and tripling of the maximum rate of heat evolution in mixtures by increasing the test temperature from 20 to 30 °C (Fig. 9) leads to different rates of setting, hydration product morphology, and strength development during installation of castable products, and highlights the importance of temperature control during castable installation. Optimisation of the parameters such as temperature, ultimate mixing, and composition to control the rate and amount of hydrotalcite formation in such castables is clearly essential.

5. Conclusions

1. Using ICC the rate and total heat evolution from the hydration of alumina (Actibond 102), reactive magnesia and mixtures of alumina-magnesia were determined up to 22 h at 20 and 30 °C.

2. Hydratable alumina (Actibond 102) reacted to only ca. 45% theoretical to form bayerite, while magnesia was almost fully hydrated to brucite after 22 h at both 20 and 30 °C.

3. The product of hydration of alumina-magnesia mixtures was a hydrotalcite-type hydrate and its formation was associated with a massive total heat evolution of ~600 kJ/kg.

4. The presence of magnesia promoted the hydration of alumina, probably by a localised temperature rise due to hydrotalcite formation. Maximum heat was released from the sample with Al_2O_3:MgO ratio of 35:65. XRD showed that some brucite existed alongside the hydrotalcite in hydration products of compositions up to an Al_2O_3:MgO ratio of 75:25. Therefore, thorough mixing of these powders might release further heat on hydration.

5. Hydration provides a microstructure, which on dehydration yields a network of micro-pores in a castable bond system. These micro-pores can direct the vapour to the outside of the body, accommodate any products formed on dehydration, and also compensate for the expansion, e.g. from spinel formation at higher temperatures.

Acknowledgements

We would like to thank EPSRC for financial support under grant No. GR/157852 and Alcan Chemicals Ltd. for supplying raw materials. We are grateful to K.J.D. MacKenzie, M. Warman and F. Azizian for useful discussions.

References

1. Banerjee, S., Recent developments in monolithic refractories. *Bull. Am. Ceram. Soc.,* 1998, **77**(10), 59–63.
2. Windle, C. J. and Bentley, V. K., Rebonded magnesia–alumina spinel products for oxy-fuel and alkali saturated atmospheres. In *Proceedings of Unified International Technical Conference on Refractories, UNITECR'99*, Berlin, Germany, 1999, pp. 219–225.
3. Korgul, P., Wilson, D. R. and Lee, W. E., Microstructural analysis of corroded alumina-spinel castable refractories. *J. Eur. Ceram. Soc.,* 1997, **17**, 77–84.
4. Fujii, K., Furusato, I. and Takita, I., Composition of spinel clinker for teeming ladle casting material. In *Proceedings of Unified International Technical Conference on Refractories, UNITECR'91*, Aachen, Germany, 1991, pp. 108–110.
5. Sarpoolaky, H., Zhang, S., Argent, B. B. and Lee, W. E., Influence of grain phase on slag corrosion of low cement castable refractories. *J. Am. Ceram. Soc.,* 2001, **84**(2), 426–434.
6. Cunha, F. N. and Bradt, R.C., Reactions of constituents for *in situ* bonds of $MgAl_2O_4$, Mg_2SiO_4 and $3Al_2O_3.2SiO_2$ in refractories. In *ISS-57th Electric Furnace Conference*, Pittsburgh, Pa, USA, 1999, pp. 143–152.
7. Parr, C., Bier, T. A., Vialle, M. and Revais, C., An approach to formulate spinel forming castables. In *Proceedings of Unified International Technical Conference on Refractories, UNITECR'99*, Berlin, Germany, 1999, pp. 19–21.
8. Sandberg, B., Myhre, B. and Holm, J. L., Castables in the system $MgO–Al_2O_3–SiO_2$. In *Proceedings of Unified International Technical Conference on Refractories, UNITECR'95*, Kyoto, Japan, 1995, pp. 173–181.
9. Forrester, J. A., A conduction calorimeter for the study of cement hydration. *Cem. Technol.,* 1970, **1**, 95–99.
10. Edmonds, R. N. and Majumdar, A. J., The hydration of monocalcium aluminate at different temperatures. *Cem. Concr. Res.,* 1988, **18**, 311–320.
11. Ma, W. and Brown, P. W., Mechanisms of reaction of hydratable aluminas. *J. Am. Ceram. Soc.,* 1999, **82**, 453–456.
12. Brindley, G. W. and Kikkawa, S., A crystal-chemical study of Mg, Al and Ni, Al hydroxy-perchlorates and hydroxy-carbonates. *Am. Mineral.,* 1979, **64**, 836–843.
13. Miyata, S., Physico-chemical properties of synthetic hydrotalcites in relation to composition. *Clays and Clay Minerals,* 1980, **28**, 50–55.
14. Pesic, L., Salipurovic, S., Markovic, V., Vucelic, D., Kagunya, W. and Jones, W., Thermal characteristics of a synthetic hydrotalcite-like material. *J. Mater. Chem.,* 1992, **2**, 1069–1073.
15. MacKenzie, K. J. D., Meinhold, R. H., Sherriff, B. L. and Xu, Z., ^{27}Al and ^{25}Mg solid-state magic-angle spinning nuclear magnetic resonance study of hydrotalcite and its thermal decomposition sequence. *J. Mater. Chem.,* 1993, **3**, 1263–1269.
16. Lee, W. E. and Rainforth, W. M., *Ceramic Microstructures, Property Control by Processing*. Chapman and Hall, London, UK, 1994.
17. Jaworska-Galas, Z., Janiak, S., Mista, J., Wrzyszcz, J. and Zawadzki, M., Morphological and phase changes of transition aluminas during their rehydration. *J. Mater. Sci.,* 1993, **28**, 2075–2078.
18. Ahari, K. G., Lee, W. E. and Habesch, S., Environmental scanning electron microscopy of hydrated refractory oxides. *Inst. Phys. Conf. Ser.* No. 161: Section 8 Institute of Physics, UK, 1999, pp. 373–376.
19. Taylor, H. F. W., Crystal structures of some double hydroxide minerals. *Mineral Mag.,* 1973, **39**, 377–388.
20. Hwang, K. H., Oh, K. D. and Bradt, R. C., In situ spinel bond formation (expansion/ contraction) during firing. In *Proceedings of the Unified International Technical Conference on Refractories, UNITECR'97*, New Orleans, USA, 1997, pp. 1575–1580.